

# A NOVEL APPROACH TO ROBUST MOTION CONTROL OF ELECTRICAL DRIVES WITH MODEL ORDER UNCERTAINTY

Stephen J Dodds

*School of computing and technology  
University of East London  
Longbridge Road, Dagenham, Essex RM8 2AS, UK  
Tel: +44 208 223 2367  
E-mail: [stephen.dodds@spacecon.co.uk](mailto:stephen.dodds@spacecon.co.uk)*

**Summary** A novel approach to the control of plants with model order uncertainty as well as parametric errors and external disturbances is presented, which yields a specified settling time of the step response with zero overshoot. The method is applied to a motion control system employing a permanent magnet synchronous motor. A single controller is designed to cater for mechanical loads that may exhibit significant vibration modes. The order of the complete controlled system (i.e., the plant) will therefore depend on the number of significant vibration modes. The controller is of the cascade structure, comprising an inner drive speed control loop and an outer position control loop. The main contribution of the paper is a completely new robust control strategy for plants with model order uncertainty, which is used in the outer position control loop. Its foundations lie in sliding mode control, but the set of output derivatives fed back extend to a maximum order depending on the maximum likely rank of the plant, rather than its *known* rank. In cases where the maximum order of output derivative exceeds the plant rank, in theory, virtual states are created that raise the order of the closed-loop system while retaining the extreme robustness properties of sliding mode control. Algebraic loops (caused by zero or negative rank of the open-loop system) are avoided by embodying filtering with a relatively short time constant in the output derivative approximations. The speed control loop is also new. Although it is based on the forced dynamic vector control principle, already developed by the author and co-researchers for drives with current fed inverters, for the first time, a version for voltage fed inverters is presented with a view to future implementation of space vector modulation to improve the smoothness of the stator current waveforms. The new forced dynamic control law requires an estimate of the load torque and its first derivative and a special observer is presented for this purpose. An initial evaluation of the method is made by considering three plants with different orders and ranks, the first being the unloaded drive, the second being the drive controlling the motor rotor angle with a mass-spring load attached and the third being the drive controlling the load mass angle of the same attached mass-spring load. The simulations indicate that the control system does indeed yield robustness including plant order uncertainty and further investigations, both theoretical and experimental, are recommended.

## 1. INTRODUCTION

A desirable property of automatic control systems is robustness, which traditionally means maintenance of closed-loop stability despite a) uncertainties or changes in the plant with respect to the plant model used for the design of the controller and b) external disturbances. These uncertainties can include the order of the plant. For example, any mechanism of a motion control system is composed of materials that have elasticity. This combines with the mass of the material to yield vibration modes, each of which adds two to the order of the system. It is quite common to assume that such mechanisms approximate rigid-body dynamics and so the vibration modes are ignored. In such cases, care must be taken not to set the controller gains too high for fear of undesirable closed loop system oscillatory modes or even instability. On the other hand, the aforementioned property of robustness cannot be expected with relatively low gain settings.

Sliding mode control [1] is a well known technique for achieving robustness but it relies effectively on extremely high gains to achieve robustness, but only with respect to external disturbances and uncertainties in the parameters of a plant model of known form. This method, as it stands, cannot achieve robustness with respect to plant model order uncertainty but when the model order is known, it not only achieves stability but can achieve a specified closed-loop dynamic response that does not change significantly in the presence of

parametric changes or external disturbances. It is also applicable to nonlinear plants.

Another well known robust control technique is to design a linear controller in the frequency domain using the  $H_\infty$  method [2]. This does not deliberately use high gains and accommodates model order uncertainty while guaranteeing closed-loop stability but, in general, yields a closed-loop dynamic response that can change significantly with the plant parameters and may exhibit some sensitivity to external disturbances.

This paper presents, for the first time, an approach that attempts to combine the best features of the two aforementioned robust control techniques. It aims to yield robustness according to the following definition:

*A control system is robust if it maintains a specified dynamic performance when a) the plant parameters are changed b) the order of the plant is changed, and c) external disturbances are applied.*

The method stems from sliding mode control and is essentially very simple. In fact, it was discovered as a result of an experiment on sliding mode control that worked successfully despite an error that violated the conventional rules of control theory. In order to describe this situation, the sliding mode control method will be briefly described. Figure 1 shows the general block diagram of a sliding mode control system designed to yield a precisely defined closed-loop dynamic performance for a single input, single output (SISO) plant.

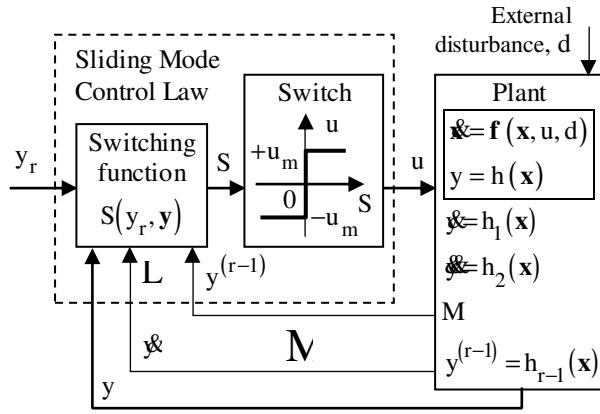


Fig. 1 General SISO sliding mode control system

There are many different forms of sliding mode control system, but this one will suffice for the purpose of this paper. Here,  $\mathbf{x} = [x_1 \ x_2 \ \dots \ x_n]^T$ , is the state vector, where  $n$  is the order of the plant, and  $\mathbf{y} = [y \ \dot{y} \ \dots \ y^{(r-1)}]^T$  is the vector of output derivatives. The rank (or relative degree) of the plant is  $r$ , such that the  $r^{\text{th}}$  output derivative is  $y^{(r)} = h_r(\mathbf{x}, u)$  and is *not* a state variable because of its dependence on the control input,  $u$ . The elements of  $\mathbf{y}$  are *all state variables* and the set of equations for the derivatives of  $y$  constitute a transformation to a new set of state variables. As can be seen, the sliding mode control law is a bang-bang control law in which  $u$  switches between maximum and minimum values of  $\pm u_m$  when  $S$  passes through zero. The switching surface,  $S(y_r, \mathbf{y}) = 0$ , is designed such that over the normal range of operating states,  $u$  is automatically switched to the value that drives  $\mathbf{y}$  towards the surface. In this way,  $\mathbf{y}$  is held on the surface while  $u$  rapidly switches between  $+u_m$  and  $-u_m$ , in theory at an infinite frequency and with a continuously varying mark-space ratio. Under these circumstances, the point,  $\mathbf{y}$ , in the output derivative space appears to *slide* in the surface and the system is said to be operating in a *sliding mode*. Also, during this *sliding motion*, the closed-loop system is governed by the differential equation,  $S(y_r, \mathbf{y}) = 0$ , i.e.,

$$S(y_r, \mathbf{y} \ \&L \ y^{(r-1)}) = 0. \quad (1)$$

Remarkably, if the switching function,  $S(y_r, \mathbf{y})$ , is linear, i.e.,

$$S(y_r, \mathbf{y}) = y_r - (y + q_1 \dot{y} + q_2 \ddot{y} + \dots + K + q_{r-1} y^{(r-1)}),$$

then the closed loop system is linear with transfer function

$$\frac{y(s)}{y_r(s)} = \frac{1}{1 + s q_1 + s^2 q_2 + \dots + K + s^{r-1} q_{r-1}} \quad (2)$$

which is *independent of the plant parameters and the external disturbance*. Furthermore, the coefficients,  $q_1, q_2, \dots, q_{r-1}$ , may be chosen independently to design the system by pole assignment to achieve *any desired dynamic performance*, within the limitations of the hardware. It must also be realised that this performance is only attained while in sliding motion. The condition for sliding motion is that the point,  $\mathbf{y}$ , in the  $r$  dimensional space with components,  $y_r, y, \dot{y}, \dots, y^{(r-1)}$ , is driven back towards the switching surface (1) from both sides by the control law. This is expressed mathematically as

$$S \dot{S} < 0 \quad (3)$$

This condition will only be satisfied over a finite region of the switching surface and, in general, this region may be increased in size by increasing the maximum control level,  $u_m$ .

The sliding mode control system described above is a state feedback control system. If the plant is of full rank, then  $r = n$  and  $\mathbf{y} = [y \ \dot{y} \ \dots \ y^{(n-1)}]^T$  is a complete state vector, enabling complete control of the plant according to standard control theory. If, however, the plant is not of full rank, i.e.,  $r < n$ , then the sliding mode control law can only control a subsystem of the plant with the state variables,  $y_r, y, \dot{y}, \dots, y^{(r-1)}$ . There then exists an uncontrolled subsystem of order,  $n - r$ . The dynamics of this uncontrolled subsystem is referred to as the *zero dynamics*. In fact, a linear plant with transfer function,  $\frac{y(s)}{u(s)} = \frac{N(s)}{D(s)}$ , which is not of full rank has  $n - r$  zeros and the pole characterising the zero dynamics are roots of  $N(s) = 0$ , i.e., the plant *zeros*. The phenomenon of zero dynamics will be seen in one of the plants considered later.

## 2. OUTPUT DERIVATIVE FEEDBACK ROBUST CONTROL LAW

According to standard control theory, it is unnecessary to feed back to the control law more variables than those constituting a complete set of plant state variables. This is because the plant state contains all the information about its present dynamic behaviour. In particular, attempting to feed back variables such as  $y^{(r)} = h_r(\mathbf{x}, u)$  or higher derivatives of  $y$  is really considered 'against the rules' because of the creation of algebraic loops through their dependence on  $u$  and its derivatives. The control technique presented in the following section, however, originated from an attempt at sliding mode position control of a d.c. motor in which the shaft angular acceleration (*not* a state variable) was

fed back as well as the shaft angular velocity and position. This system is shown in Figure 2.

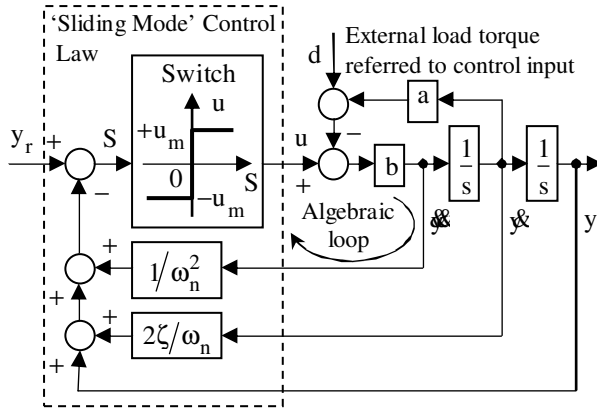


Fig. 2 An attempt at sliding mode control with one higher output derivative than necessary

Despite the violation of the general rule that all the variables fed back to the control law should be state variables (causing the algebraic loop shown), the system operated correctly. This may be demonstrated as follows. When  $S \equiv 0$ , the switch operates similarly to a high gain. In fact, a well-known technique for eliminating the undesirable rapid switching of  $u$  in the sliding mode is to replace the switch by a high gain,  $K$ . Then as  $K \rightarrow \infty$ ,  $u \rightarrow u_{eq}$ , which is the continuous control equivalent to the aforementioned control switching at infinite frequency with continuously varying mark-space ratio, in that it produces precisely the same effect. This is called the *equivalent control*. Replacing the switch by a gain,  $K$ , in Figure 2 yields the following closed-loop transfer function relationship, with the aid of Mason's formula:

$$y(s) = \frac{\omega_n^2 y_r(s) - \frac{1}{K} \omega_n^2 d(s)}{\frac{\omega_n^2}{Kb} s^2 + (s^2 + 2\zeta\omega_n s + \omega_n^2) + \frac{ab}{K} s\omega_n^2}$$

It is now evident that as  $K \rightarrow \infty$ , then

$$\lim_{K \rightarrow \infty} y(s) = \left( \frac{\omega_n^2}{s^2 + 2\zeta\omega_n s + \omega_n^2} \right) y_r(s) \quad (4)$$

Hence any desired second order system response can be obtained by suitable choice of the feedback gains,  $q_1 = 2\zeta/\omega_n$  and  $q_2 = 1/\omega_n^2$ .

Now the proposed control law is simply that of Figure 1 without any restriction on the order of the output derivatives being fed back and with the switch replaced by the gain,  $K$ . In this case,  $S(y_r, y)$  will be called simply the *sliding function* since there is no switch. It is shown in Figure 3 for a linear plant and a linear sliding function.

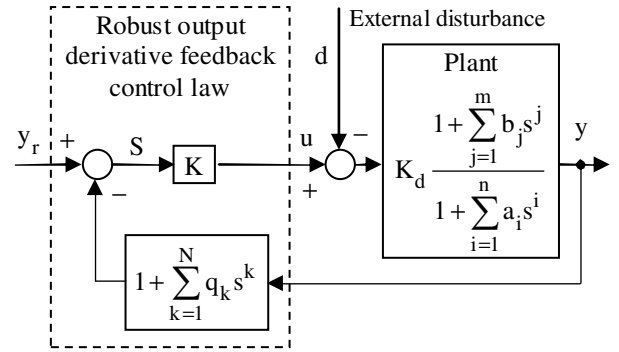


Fig. 3 Linear output derivative robust control law applied to a linear plant

The closed-loop transfer function relationship is now

$$y(s) = \frac{K_d \left( 1 + \sum_{j=1}^m b_j s^j \right) \left[ y_r(s) - \frac{1}{K} d(s) \right]}{\frac{1}{K} \left( 1 + \sum_{i=1}^n a_i s^i \right) + K_d \left( 1 + \sum_{k=1}^N q_k s^k \right) \left( 1 + \sum_{j=1}^m b_j s^j \right)}$$

It is evident that the order,  $n_c$ , of the closed-loop system is given by

$$n_c = \begin{cases} n & \text{if } N + m \leq n \\ N + m & \text{if } N + m > n \end{cases} \quad (5)$$

If  $N + m > n$ , then the following limit can be taken:

$$\lim_{K \rightarrow \infty} y(s) = \frac{1}{1 + \sum_{k=1}^N q_k s^k} \cdot y_r(s) \quad (6)$$

The system can then be designed by pole assignment but in the above limit, the closed loop characteristic equation becomes:

$$\left( 1 + \sum_{k=1}^N q_k s^k \right) \left( 1 + \sum_{j=1}^m b_j s^j \right) = 0 \quad (7)$$

and therefore  $m$  of the closed-loop poles are the zeros of the plant transfer function, which cannot be changed and it is essential that all of these poles are in the left half of the  $s$ -plane. It is evident that the order of the closed-loop system increases beyond the plant order,  $n$ , by an amount equal to the number of output derivatives that do not qualify as state variables.

If now plant model order uncertainty is considered, it is supposed that it is possible to choose an upper limit,  $r_{\max}$ , of the plant rank, which the real plant is guaranteed not to exceed. Then the controller can be designed with  $N = r_{\max}$ .

In fact, the controller will produce the same closed-loop performance, according to (6), for a whole range of different plants of rank ranging between 1 and  $r_{\max}$ .

### 3. A ROBUST POSITION CONTROL SYSTEM BASED ON A FORCED DYNAMIC VECTOR CONTROLLED PSM DRIVE

In this section a motion control system will be developed for simulation study of the new robust control technique. This comprises a vector controlled PMSM driving a mechanical load of variable order and rank. First the mechanism will be described and modelled. Then the vector control law implementing the speed control loop be developed. Finally a practicable version of the robust output derivative control law will be formulated. Figure 4 shows an overall block diagram of the motion control system.

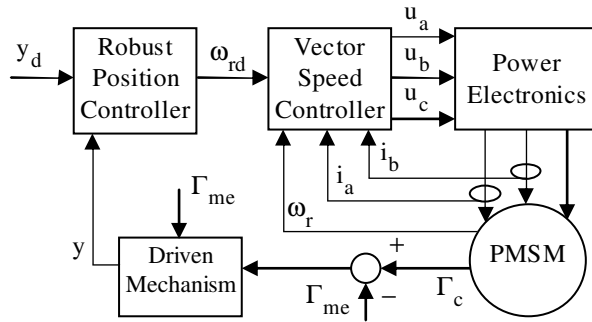


Fig. 4 Motion control system for simulation study

All the variables shown are defined in the following.

#### 3.1 Driven mechanism

The driven mechanism is a balanced mass with moment of inertia,  $J_L$ , coupled to the motor shaft via a torsion spring with spring constant,  $K_s$ , as shown in Figure 5.

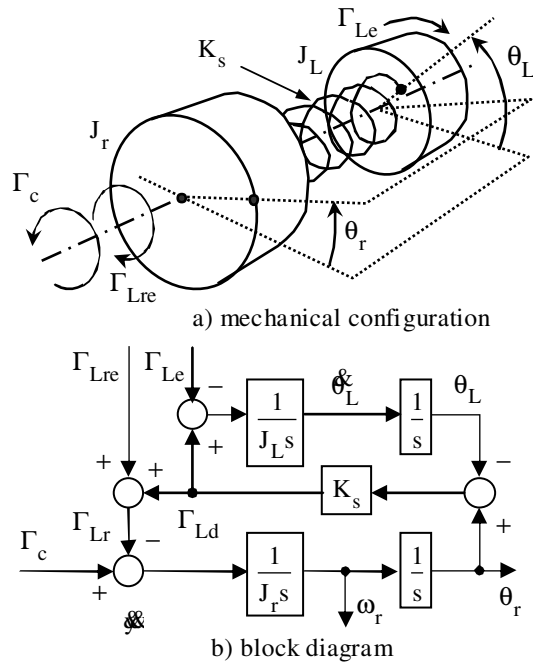


Fig. 5 Model of the driven mechanism

The corresponding torque balance equations are as follows:

$$J_r \ddot{\theta}_r = \Gamma_c - \Gamma_{Lre} + K_s (\theta_L - \theta_r) \quad (8a)$$

$$J_L \ddot{\theta}_L = K_s (\theta_r - \theta_L) - \Gamma_{Le} \quad (8b)$$

where  $J_r$  is the rotor moment of inertia,  $\theta_r$  is the rotor angle,  $\theta_L$  is the load mass angle,  $\Gamma_{Lre}$  and  $\Gamma_{Le}$  are the external load torques applied, respectively, to the rotor and the load mass and  $\Gamma_c$  is the control torque produced by the motor.

#### 3.2 Vector speed controller

The permanent magnet SM is modelled in the synchronously rotating d-q co-ordinate system by the following set of three state differential equations:

$$\frac{di_d}{dt} = -A i_d + B \omega_r i_q + F u_d \quad (9a)$$

$$\frac{di_q}{dt} = -C \omega_r i_d - D i_q - E \omega_r + G u_q \quad (9b)$$

$$\frac{d\omega_r}{dt} = (H + K i_d) i_q - M \Gamma_{Lr} \quad (9c)$$

where  $i_d$ ,  $i_q$  and  $u_d$ ,  $u_q$  are the stator current and voltage components,  $\omega_r$  is the rotor angular velocity and  $\Gamma_{Lr}$  is the net rotor load torque.

The constant coefficients are

$$\begin{cases} A = R_s/L_d; B = pL_q/L_d; C = pL_d/L_q; D = R_s/L_q; \\ E = p\Psi_{PM}/L_q; F = 1/L_d; G = 1/L_q; \\ H = 3p\Psi_{PM}/(2J_r); K = 3p(L_d - L_q)/(2J_r); M = 1/J_r \end{cases}$$

where  $\Psi_{PM}$  is the permanent magnet flux,  $R_s$  is the stator resistance,  $L_d$  and  $L_q$  are the direct and quadrature axis inductances, and  $p$  is the number of pole pairs.

A forced dynamic control law [3] will now be derived. The two controlled variables are  $\omega_r$  and  $i_d$  (controlled with a zero reference input,  $i_{dd} = 0$ , to keep the current and magnetic field vectors mutually perpendicular, for maximum torque efficiency).

The rank with respect to  $i_d$  is just 1 and so the desired closed loop differential equation may be written:

$$\frac{di_d}{dt} = \frac{3}{T_{si}} (i_{dd} - i_d) \quad (10)$$



The fact that Plants 1 and 2 are identical and independent of the rotor external load torque,  $\Gamma_{Lre}$ , is due to the robustness already given by the forced dynamic speed control law (15), through the terms,  $\hat{\Phi}_L$  and  $\hat{\omega}_r$  compensating the time varying net rotor load torque,  $\Gamma_{Lr}$  in Figure 5, artificially decoupling the mass-spring load from the system. The plants presented to the complete controller are different from one another. From Figure 5:

Plant 1 (Dynamic load torque,  $\Gamma_{Ld}$  removed):

$$\theta_r(s) = \frac{\Gamma_c(s) - \Gamma_{Lre}(s)}{J_r s^2} \quad (20)$$

Plant 2:

$$\theta_r(s) = \frac{\frac{1}{J_r} \left[ \left( s^2 + \frac{K_s}{J_L} \right) (\Gamma_c(s) - \Gamma_{Lre}(s)) - \frac{K_s}{J_L} \Gamma_{Le}(s) \right]}{s^2 \left( s^2 + \frac{K_s}{J_r} + \frac{K_s}{J_L} \right)} \quad (21)$$

Plant 3:

$$\theta_r(s) = \frac{\frac{1}{J_L} \left[ \frac{K_s}{J_r} (\Gamma_c(s) - \Gamma_{Lre}(s)) - \left( s^2 + \frac{K_s}{J_r} \right) \Gamma_{Le}(s) \right]}{s^2 \left( s^2 + \frac{K_s}{J_r} + \frac{K_s}{J_L} \right)} \quad (22)$$

With reference to (18) and (19), the maximum rank is  $r_{max} = 5$ . Figure 7 shows a block diagram of the outer robust position control loop for this case corresponding to Figure 3, with low-pass measurement noise filtering, with a time constant,  $T_f = T_s$  where  $T_s$  is the settling time.

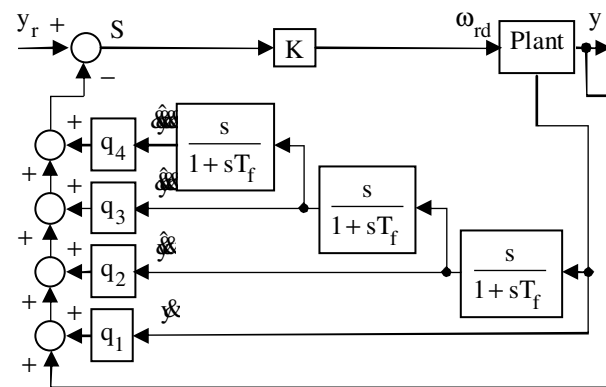


Fig. 7 Outer robust control loop for simulation

It is assumed that, as is usual in electrical drives the angular velocity measurements,  $\omega_r$  and  $\hat{\omega}_L$ , are both available, so that only three approximate differentiations are necessary in the controller.

The output derivative feedback gains,  $q_1$  to  $q_4$  are determined by pole assignment, using the author's

settling time formula,  $T_s = 1.5(1+N)T_c$ , for a linear system with coincident poles at  $s = -1/T_c$ . In this case

$$\frac{y(s)}{y_r(s)} = \frac{1}{1 + q_1 s + q_2 s^2 + K q_N s^N} = \frac{1}{\left( 1 + s \frac{T_s}{1.5(1+N)} \right)^N}$$

where  $N = r_{max} - 1 = 4$ . Thus:

$$\begin{cases} q_1 = 4 \cdot \left( \frac{2T_s}{15} \right) & q_2 = 6 \cdot \left( \frac{2T_s}{15} \right)^2 \\ q_3 = 4 \cdot \left( \frac{2T_s}{15} \right)^3 & q_4 = \left( \frac{2T_s}{15} \right)^4 \end{cases} \quad (23)$$

#### 4. SIMULATIONS

The PMSM parameters taken are as follows:

$J_r=0.003 \text{ Kg m}^2$ ;  $p=3$ ;  $L_d=1.4 \text{ H}$ ;  $L_q=0.1618 \text{ H}$ ;  $R_s=36.5 \text{ } \Omega$ ;  $\Psi_{PM}=0.312 \text{ Wb}$ .

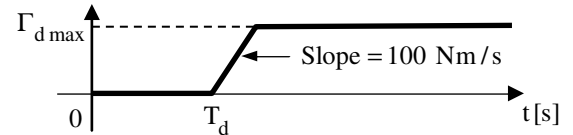
The Mechanical load parameters for plants 2 and 3 are:

$J_L=0.01 \text{ Kg m}^2$ ;  $K_s=9 \text{ Nm/rad}$

The forced dynamic control law parameters are set to

$T_s=0.2$ ;  $K=200$ ;  $T_f = 0.0001s$ ;  $T_{so} = 0.001s$ ;  $T_s = 0.2s$  with the derivative feedback gains according to (22).

For all three plants, a step reference angle of 2 rad was applied. The robustness against external disturbances was tested by applying external load torques according to Figure 8.



	Plant 1	Plants 2 and 3
$\Gamma_{Lre}$ [Nm]	$\Gamma_{d \max} = 3 \text{ Nm}$ $T_d = 0.5 \text{ s}$	$\Gamma_{d \max} = 3 \text{ Nm}$ $T_d = 0.5 \text{ s}$
$\Gamma_{Lc}$ [Nm]	Not applicable	$\Gamma_{d \max} = 1 \text{ Nm}$ $T_d = 1 \text{ s}$

Fig. 8 External load torques for simulation

Figures 9 to 16 show simulations without mismatching of the PMSM parameters.

It is evident from Figure 9 that the system is very robust with respect to changes in the driven mechanical load and to both load torques.

Figures 10 11 and show, respectively, the load torque and load torque derivative being very accurately estimated by the observer for Plant 1. The initial accelerating and decelerating control torque is clearly

visible in Figure 10, after which the control torque closely follows the load torque in order to counteract it.

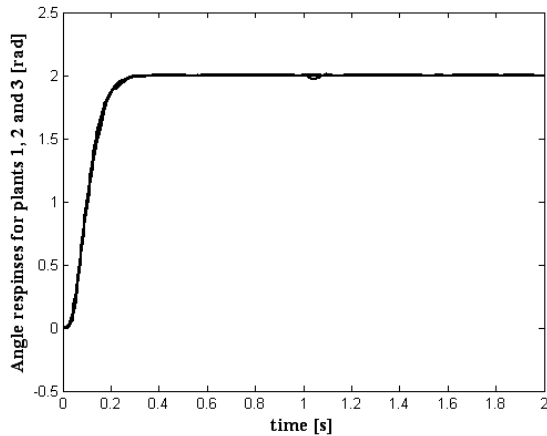


Fig. 9 Angle step responses of Plants 1, 2 and 3

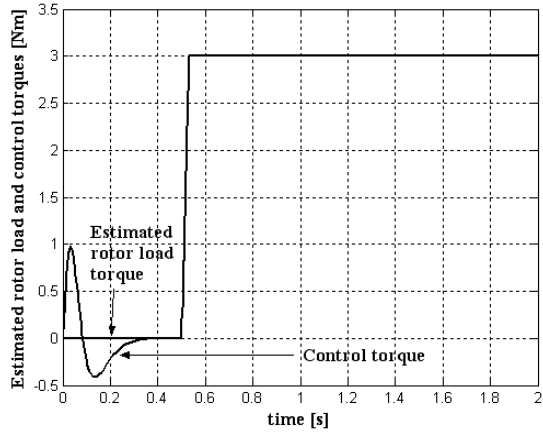


Fig. 10 Estimated load and control torques for Plant 1

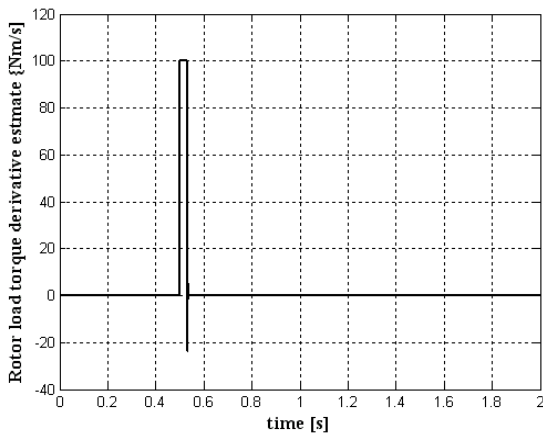


Fig. 11 Load torque derivative estimate for Plant 1

Figure 12 shows the three-phase stator currents with similar shape to the control torque of Figure 10, as expected.

Figure 13 shows the rotor angle for Plant 2 being very accurately controlled while the sprung load mass is uncontrolled and left to oscillate. This is a consequence of the dynamic load torque,  $\Gamma_d$ , being counteracted by the forced dynamic inner loop speed controller, which is evident in Figure 14, where the

oscillatory net load torque is being followed closely by the control torque. This result is expected with the

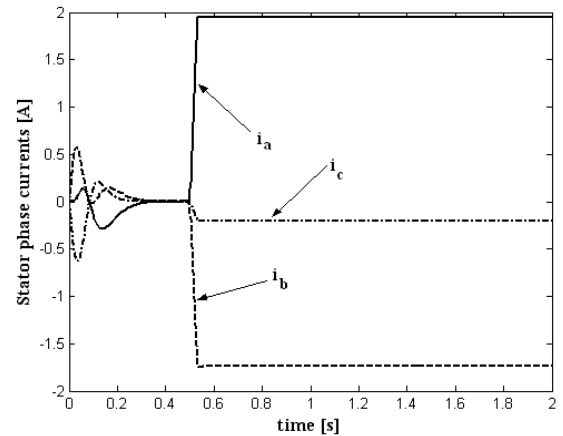


Fig. 12 Stator phase currents for Plant 1

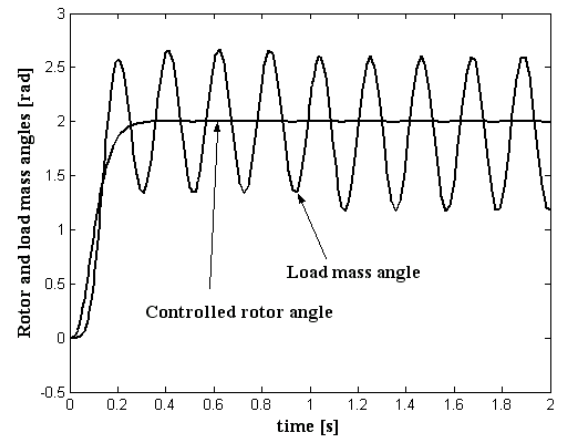


Fig. 13 Plant 2 rotor and load mass angles

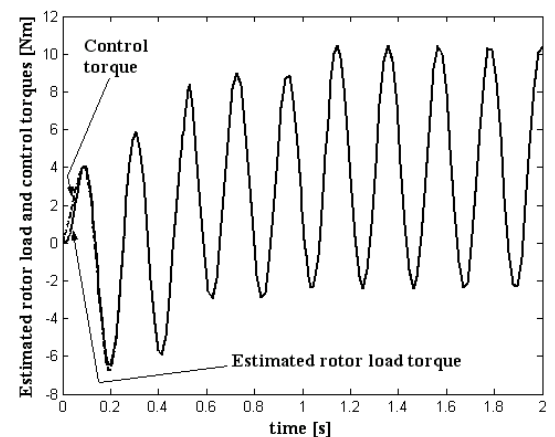


Fig. 14 Estimated load and control torques for plant 2

controller as designed, since it is intended to control the rotor angle. Further development of the robust controller would be needed in order to achieve active damping of the sprung load mass oscillations while satisfactorily controlling the rotor angle. This would have to be a compromise, however, since the oscillatory damping torques would have to be provided by the motor (via the spring) and therefore would affect the settling time and accuracy of the rotor angle control.

Figure 15 shows the sprung load mass angle being accurately controlled while rotor angle is moved by the

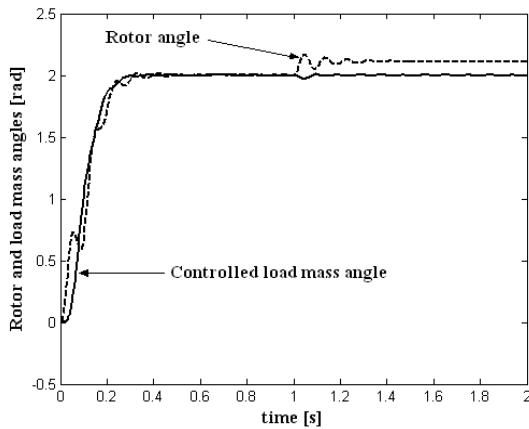


Fig. 15 Plant 3 rotor and load mass angles

controller to apply the necessary control torques to the sprung mass via the spring. In contrast to Plant 2, Plant 3 is of full rank (no transfer function zeros) and this explains the stable behaviour of the whole system.

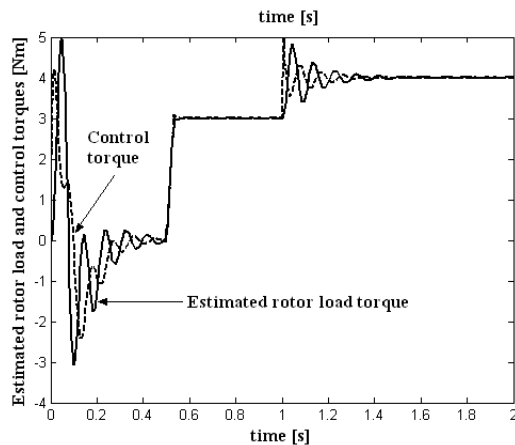


Fig. 16 Estimated load and control torques for plant 3

Figure 16 shows the difference between the control torque and net load torque needed to accelerate and decelerate the load mass while keeping the oscillations under control. Also, the responses of the load torque estimate to the two external load torques is visible.

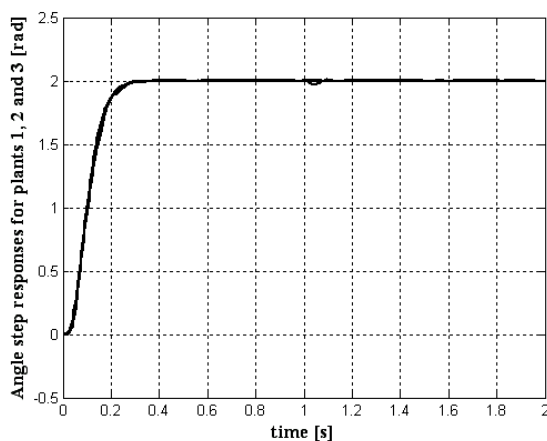


Fig. 17 Responses: +50% rotor m.o.i. error

Figure 17 shows the responses of all three plants when the rotor moment of inertia is over-estimated by 50%. The remarkable degree of robustness is achieved by the forced dynamic controller, since such an error in the rotor moment of inertia is equivalent to an added (or subtracted) rotor mass, reflected by a change in the dynamic load torque,  $\Gamma_{Ld}$ , (ref., Figure 5), which is estimated by the observer and counteracted by the controller.

Finally, Figure 18 shows the responses obtained with the following worst-case mismatching of the assumed PMSM parameters:

$J_r$ ,  $L_d$  and  $L_q$  overestimated by 10%.

$R_s$  and  $\Psi_{PM}$  underestimated by 10%.

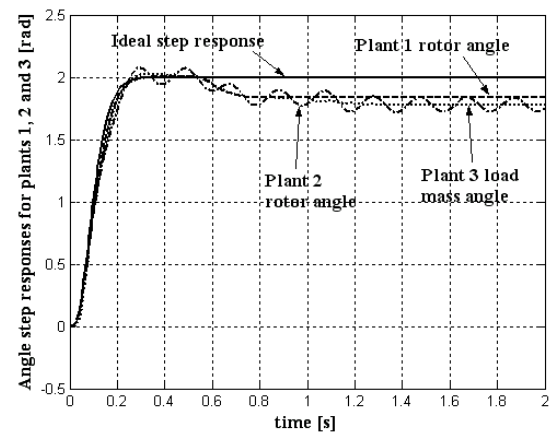


Fig. 18 Responses: worst-case 10% parameter errors

All three plants are kept under control, but not so accurately. This is due to the control torque input to the observer depending on accurate estimates of  $\Psi_{pm}$ ,  $L_d$  and  $L_q$ , as can be seen in Figure 6.

## 5. CONCLUSIONS AND SUGGESTIONS FOR FURTHER WORK

The simulations carried out indicate that the new robust output derivative controller is capable of controlling the selected third and fifth order plants with the same specified dynamic responses, in the presence of external disturbances. It is therefore recommended that the technique is investigated for a much wider range of plants.

Although the PMSM drive simulation included the complete vector control algorithm with the 2/3 and 3/2 phase transformations, the power electronic switching was not included and this should be done together with some experiments.

## REFERENCES

- [1] Utkin, V. I., *Sliding Modes in Control and Optimisation*, Springer Verlag, 1992.
- [2] Zhou, K., Doyle, J. C. and Glover, K., *Robust and Optimal Control*, Prentice Hall, 1996.
- [3] Vittek, J., Dodds, S. J., *Forced Dynamics Control of Electric Drives*, University of Zilina Press, 2003, ISBN 80-8070-087-7.